A Method to Estimate the Oblique Arch Folding Axis for Thumb Assistive Devices

Nanayakkara, Visakha K., Nantachai Sornkaran, Hasitha Wegiriya, Nikolaos Vitzilaios, Demetrios Venetsanos, Nicolas Rojas, M. Necip Sahinkaya, and Thrishantha Nanayakkara

Original citation & hyperlink:
Nanayakkara, V.K., Sornkaran, N., Wegiriya, H., Vitzilaios, N., Venetsanos, D., Rojas, N., Sahinkaya, M.N. and Nanayakkara, T., 2019, July. A method to estimate the oblique arch folding axis for thumb assistive devices. In *Lecture Notes in Computer Science*, Vol.11649 (pp. 28-40). Springer, Cham. https://dx.doi.org/10.1007/978-3-030-23807-0_3

DOI 10.1007/978-3-030-23807-0_3
ISSN 0302-9743
ESSN 1611-3349

Publisher: Springer

The final publication is available at Springer via http://dx.doi.org/10.1007/978-3-030-23807-0_3

A method to estimate the oblique arch folding axis for thumb assistive devices

Visakha K. Nanayakkara[1], Nantachai Sornkaran[2], Hasitha Wegiriya[2], Nikolaos Vitzilaios[3], Demetrios Venetsanos[4], Nicolas Rojas[5], M. Necip Sahinkaya[6], and Thrishantha Nanayakkara[5]

[1]Mechanical Engineering Department, CEMAST Campus, Fareham, PO13 9FU, UK
{visakha.nanayakkara}@fareham.ac.uk
[2] Department of Informatics, King's College London
{nantachai.sornkarn, hasitha.wegiriya}@kcl.ac.uk
[3]Department of Mechanical Engineering, University of South Carolina, SC, USA
{VITZILAIOS}@sc.edu
[4] School of Mechanical, Aerospace and Automotive Engineering, Coventry University, UK
{ac6109}@coventry.ac.uk
[5] Dyson School of Design Engineering, Imperial College London, UK
{n.rojas, t.nanayakkara}@imperial.ac.uk
[6] Department of Mechanical and Automotive Engineering, Kingston University London, UK
{M.Sahinkaya}@kingston.ac.uk

Abstract. People who use the thumb in repetitive manipulation tasks are likely to develop thumb related impairments from excessive loading at the base joints of the thumb. Biologically informed wearable robotic assistive mechanisms can provide viable solutions to prevent occurring such injuries. This paper tests the hypothesis that an external assistive force at the metacarpophalangeal joint will be most effective when applied perpendicular to the palm folding axis in terms of maximizing the contribution at the thumb-tip as well as minimizing the projections on the vulnerable base joints of the thumb. Experiments conducted using human subjects validated the predictions made by a simplified kinematic model of the thumb that includes a foldable palm, showing that: 1) the palm folding angle varies from 71.5° to 75.3° (from the radial axis in the coronal plane) for the four thumb-finger pairs and 2) the most effective assistive force direction (from the ulnar axis in the coronal plane) at the MCP joint is in the range $0° < \psi < 30°$ for the four thumb-finger pairs. These findings provide design guidelines for hand assistive mechanisms to maximize the efficacy of thumb external assistance.

Keywords: Thumb kinematics, foldable palm, metacarpophalangeal joint, thumb assistance

1 Introduction

Repetitive forceful occupational tasks like handling heavy tools and pipetting are likely to cause long term musculoskeletal impairments and localized muscle tension in the thumb [7], [19]. While the thumb is found to be playing a leading role in any grasp [9], [5], it has been observed that the basal trapeziometacarpal (TM) joint of the thumb is

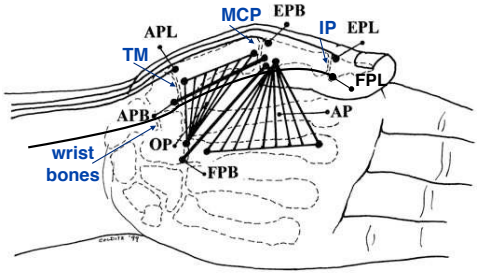

Fig. 1: Thumb muscle arrangement reprinted with kind permission from Judy Colditz [4] and modified to indicate the thumb joints and wrist bones. Three joints: trapeziometacarpal (TM), metacarpophalangeal (MCP), and interphalangeal (IP). Four extrinsic muscles: Extensor Pollicis Brevis (EPB), Abductor Pollicis Longus (APL), Extensor Pollicis Longus (EPL), Flexor Pollicis Longus (FPL). Five intrinsic muscles: Opponenes Pollicis (OP), Abductor Pollicis Brevis (APB), Flexor Pollicis Brevis (FPB), Adductor Pollicis (AP), First interossei (FI) (not shown).

loaded more than the other joints [11]. The TM joint's unique saddle shape with the wrist bone along with its distinctive muscle and ligament capsule enables substantial movements of the thumb to reach the tips of the other fingers (thumb opposition) and to stabilize any grasp [14].

The human thumb has three joints, namely TM or carpometacarpal, metacarpophalangeal (MCP), and interphalangeal (IP); five intrinsic muscles located in the palm, and four extrinsic muscles connected to the bones via tendons (Fig. 1). The main role of the palmar intrinsic muscles is to move the thumb in different opposition ranges towards the other fingers while flexing, abducting, or medially rotating the thumb proximal joints [14]. In addition, the extrinsic FPL muscle is also dedicated to flex the thumb; the other extrinsic muscles support thumb extension [4]. In this context, it is important to abstract thumb's integrated musculoskeletal arrangement with the palm in a kinematic model of the thumb [18], [13] to design any external assistance to reduce further loading when repetitive tasks are done. Since the MCP joint is more accessible and directly connected to the TM joint, it seems more suitable to provide external support towards the palm.

Some notable work done to develop thumb assistive devices so far include, a pediatric robotic thumb exoskeleton [1], an articulated parallelogram mechanism to support thumb joint Flexion-Extension (F-E) along with thumb rotation at the base [2], co-actuated RoboGlove to assist all five fingers [8], a tendon-driven, polymer-based wearable robotic hand (Exo-glove Poly) to support thumb F-E [10], and a synergy-based single actuator tendon-driven wearable glove [20]. However, the thumb assistive force direction is not clearly specified and the assistance towards the foldable palm is not investigated in detail in the assistive devices developed so far.

In this paper, we test the hypothesis that an external assistive force exerted at the MCP joint of the thumb is most effective if it is parallel to the oblique arch [16]. Hereafter, we refer to the oblique arch folding axis as the virtual palm folding axis. The effectiveness of external assistance is measured in terms of the force gain at the thumb-

tip. Since thumb's integrated musculoskeletal arrangement (Fig. 1) with a foldable palm is not in general incorporated in thumb kinematic models (e.g. [18], [3]), a previously proposed thumb kinematic model with a virtual foldable palm joint is adopted in this work to simulate the hypothesis [12]. Simplified model based predictions are tested using experiments on human subjects to understand how a supportive tendon force at the MCP joint contributes to the thumb-tip pinch grip using an assistive tendon driven glove. We observe that the effective assistive force direction range from the experimental results is within the analytically predicted range from the adopted kinematic model.

The rest of this paper is organized as follows: Section 2 elaborate the kinematic modeling and experimental methods used to test the hypothesis. The numerical simulation and experimental results are presented in section 3. Finally a discussion and concluding remarks are given in sections 4 and 5 respectively.

2 Methodology

2.1 Experiment 1: Variation of the palm folding angle across thumb-finger pairs

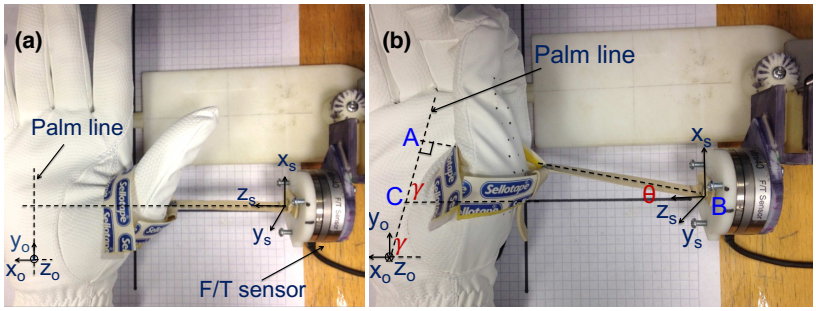

Fig. 2: Experiment 1 to evaluate palm folding angle γ. The reference $x_\circ$-$y_\circ$ axes are in the palmar coronal plane. Force sensor z_s-x_s plane conforms to the reference $x_\circ$-$y_\circ$ plane (plane of the paper). y_s and $z_\circ$ are normal to the paper. (a) Initial hand position with rubber band in tension. The palm line is taken along $y_\circ$ direction at the beginning. (b) Thumb and index finger-tip grasp posture with the moved rubber band. Virtual triangle ABC is defined on the $x_\circ$-$y_\circ$ plane, taking the rubber band projection on AB. θ is the angle of the rubber band from the z_s axis.

This experiment is conducted to estimate the palm folding angle (γ in Fig. 2(b)) based on the assumption that the MCP joint would exert a force perpendicular to the palm folding axis during a palm folding movement. Therefore, we asked human participants to move the thumb to touch each other finger with a rubber band attached between the MCP joint location of a GECKO-TAC leather glove and an ATI Mini40 (SI-40-2) 6-axis Force/Torque (F/T) transducer mounted on a fixed frame (Fig. 2). Three male and one female subjects participated in this experiment.

The initial force sensor measurement is taken when the hand is open as in Fig. 2(a) with the band in tension. This anatomical position is taken to be as the coronal plane. Then the subjects are asked to move the thumb-tip to reach each finger-tip as shown in Fig. 2(b). Palm folding angle is computed using F/T transducer measurements for these two thumb postures (Fig. 2) for the four thumb-finger pairs.

The coordinate frames are assigned as follows: Force sensor z_s-x_s space coincides with the reference $x_\circ$-$y_\circ$ space (coronal plane *ie.* the plane of the paper). y_s and $z_\circ$ are normal to the paper. In the data analysis, the force sensor y axis (y_s) is rotated around z_s to account for the force sensor misalignment. A virtual triangle ABC is defined on the plane $x_\circ$-$y_\circ$ taking the projection of the moved rubber band along AB. Hence the initial and resulting force sensor values are used to find the rubber band movement angle θ (Fig. 2(b)) for each thumb-finger combination. The palm folding arch, approximated as the line AC that goes through the reference is defined such that AB and AC are perpendicular to each other for each thumb-finger pair combination. Therefore, the palm folding angle γ (in the coronal plane) can be computed when θ is known.

2.2 Kinematic model of the thumb and foldable palm

A simplified 7-DOFs kinematic model proposed in [12] is used to ascertain how thumb-tip force gain depends on the interaction between the palm folding angle and the direction of the assistive force given at the MCP joint (Fig. 3). The coordinate frames for each joint, link connections, and design parameters of the kinematic chain are defined according to the Denavit-Hartenberg (D-H) notation (Table 1) [6].

Each consecutive thumb joint position in Fig. 3 is evaluated using link parameters and transforming frame N corresponding to the N^{th} joint to the wrist reference frame 0 using the transformation [6],

$$ {}^{0}_{N}T = \prod_{i=0}^{N-1} {}^{i}_{i+1}T \tag{1} $$

where $N = 8$.

The thumb-tip position vector is obtained from the first three elements of the last column of ${}^{0}_{N}T$ in Eq. 1. The Jacobian matrix for the thumb-tip is computed using the symbolic MATLAB function.

Table 1: D-H parameters for the thumb-palm kinematic model illustrated in Fig. 3 [12].

Joint no.	Link twist (deg)	Link length (mm)	Link offset (mm)	Joint angle (deg)
1	90	0	0	θ_1
2	-90	0	l_1	θ_2
3	-90	0	0	θ_3
4	0	l_2	0	θ_4
5	90	0	0	θ_5
6	0	l_3	0	θ_6
7	0	l_4	0	θ_7

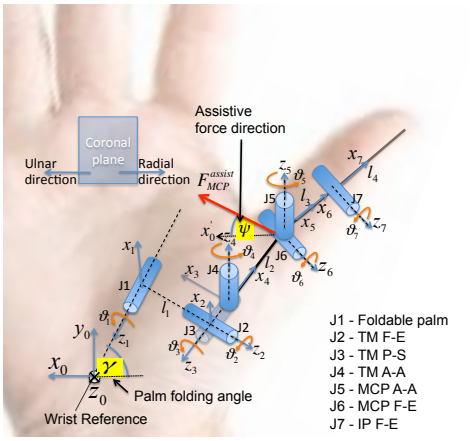

Fig. 3: 7-DOFs kinematic model of the thumb with foldable palm adopted to analyse the effective thumb assistive force direction [12]. $\theta_1 - \theta_7$ are J1-J7 joint rotational movements respectively. Thumb link lengths $l_2 - l_4$ represent thumb bone lengths whereas l_1 is the virtual orthogonal length from TM to J1 axis. Palm folding angle γ is the J1 axis inclination from the radial direction at the wrist reference (in the coronal plane). Assistive force F_{MCP}^{assist} is applied at the MCP joint at variable inclinations of ψ with respect to an axis $x_\circ^{'}$ parallel to the wrist reference $x_\circ$ in ulnar direction on the $x_\circ - y_\circ$ space.

Thumb joint angle ranges are defined based on extensive precision grasp experiments done in the previous study [12].

Joint torques τ_{pre} are calculated assuming there is an initial unit force F_{tip}^{pre} at the thumb-tip to hold an object,

$$\tau^{pre} = J_{tip}^T F_{tip}^{pre} \tag{2}$$

Similarly, joint torques τ_{assist} due to the assistive unit force F_{MCP}^{assist} exerted at the MCP at variable directions of ψ from the ulnar axis in the coronal plane (Fig. 3) are computed as,

$$\tau_{assist} = J_{MCP}^T F_{MCP}^{assist} \tag{3}$$

where τ^{pre} and τ_{assist} are 7×1 and 4×1 torque vectors respectively, J_{tip} and J_{MCP} are 3×7 and 3×4 Jacobian matrices, F_{tip}^{pre} is the 3×1 unit force vector at the thumb-tip and F_{MCP}^{assist} is the 3×1 external assistive force vector in $x - y$ space. The new thumb-tip force F_{tip}^{post} is given by,

$$F_{tip}^{post} = (J_{tip}^T)^+ (\tau_{pre} + \tilde{\tau}_{assist}) \tag{4}$$

where $(J_{tip}^T)^+$ is the pseudoinverse of J_{tip}^T (assuming full-rank) and $\tilde{\tau}_{assist} = [\tau_{assist}^T \; 0_{1\times 3}]^T$.

Assistive force gain at the thumb-tip is then evaluated by taking the ratio of the Euclidean norms of F_{tip}^{post} and F_{tip}^{pre}, that is, $|F_{tip}^{post}|/|F_{tip}^{pre}|$.

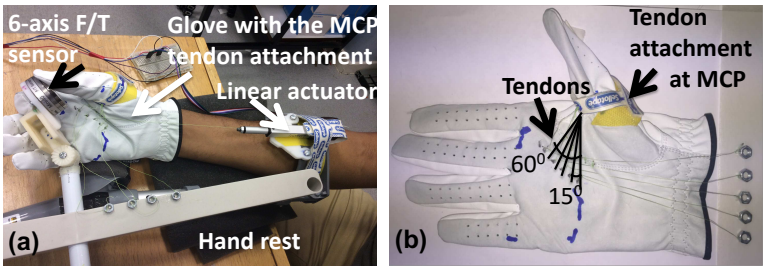

Fig. 4: Experiment 2: (a) Experimental setup to record force sensor and linear actuator data. Customized experimental setup supports the hand to keep in a flat position to obtain a consistent tendon assistance across each thumb-finger pair. (b) Wearable leather glove with attached assistive tendons to the thumb MCP joint ($0^\circ - 60^\circ$). Each tendon is 15° apart.

2.3 Experiment 2: Interaction between the palm folding angle and the thumb assistive force direction

This experiment is carried out to find how thumb-tip force gain varies for different combinations of palm folding angles and thumb assistive force directions.

Five tendons are attached to a Velcro ring fastened around the MCP joint location of a GECKO-TAC leather glove as shown in Fig. 4(a). The tendons are attached from $0^\circ - 60^\circ$ in 15° increments. These tendons are braided fishing lines of diameter 0.15 mm.

A linear actuator (L12-50-210-06-I from Firgelli Technologies Inc.) fixed to the experimental setup as shown in Fig. 4(a) controls individual tendon movement of 5 mm. Each tendon goes through a threaded pulley before it is connected to the actuator. The subjects are asked to hold an ATI Mini40 (SI-40-2) 6-axis F/T transducer which is mounted on a movable frame (Fig. 4(a)). While they are maintaining a constant pinch grip force (by looking at the force profile on the computer in front of them), an assistive force pulse (a linear tendon pull of 5 mm with duration of 5 s) is given at the MCP joint from the linear actuator. Five such pulses are given for each tendon within each thumb-finger pair trial range of 100 s with a sampling frequency of 1000 Hz. A representative raw data set is shown in Fig. 5. The linear actuator and force sensor readings are recorded for ten subjects (five male and five female), four thumb-finger pairs with five tendons for each pair using LabVIEW software, National Instruments Corp., through the data acquisition card.

All the selected subjects for both experiments 1 and 2 are right-handed and have no known thumb injuries or past thumb arthritis with their ages ranging from 25-45. Experimental procedure is approved by the Biomedical Sciences, Medicine, Dentistry and Natural and Mathematical Sciences Research Ethics Panel (BDM REP).

Recorded linear actuator assistive pulse command is smoothed out by applying a 3^{rd} order polynomial Savitzky-Golay filter with frame size 7. Time indexes of the already smoothed assistive force pulses are used to find the resultant force pulses at the thumb-tip sensor measurements (Fig. 5). Then the resultant thumb-tip force vector for each

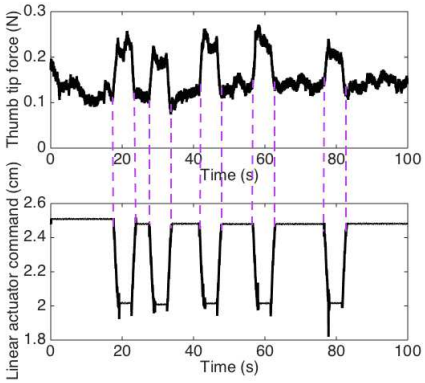

Fig. 5: A representative raw data trial. (*top*) Normal thumb-tip force including resultant pulses. (*bottom*) Corresponding linear assistive pull with five pulses plotted against time. The spikes in the linear actuator control command at the edges come from the internal control action to correct position errors in the transient phase.

pulse is computed using its 3D base vector (before the pulse) and the corresponding 3D pull vector (after the pulse). The thumb-tip force vector during the assistive pull is projected onto the thumb-tip base vector (F_b) and is added to it, to find the effective thumb-tip pull vector (F_p). The assistive force gain (F_p/F_b) is computed for each pulse taking the norms of F_p and F_b. Then the effective force gain is computed using the average force gains for the five pulses (Fig. 5).

Each input assistive force pulse at the MCP is a linear actuator pull of 5 mm for 5 s (Fig. 5) whereas, in the simulation, it is taken as a unit force vector (Fig. 3). Since thumb-tip force gain is calculated using the forces at the thumb-tip before and after exerting the assistive force at the MCP joint, the input force at the MCP is not taken into account in force gain computation.

Kolmogorov-Smirnov test is performed to check whether the force gain data for all the subject-finger-tendon pairs are normally distributed. Depending on the outcome, non-parametric Wilcoxon rank sum right-tailed, left-tailed, and two-sided (paired) hypothesis tests (equivalent to Mann-Whitney U test) are performed to test the significance of the assistive force direction across thumb-finger pairs, based on a significance level of $p < 0.05$.

3 Results

3.1 Variation of the palm folding angle (experiment 1)

Fig. 6 shows the results of experiment 1 (see methods section 2.1 for more details) suggesting that we can identify a steady state palm folding axis that varies its angle from $71.5^\circ - 75.3^\circ$ across the other four fingers. It should be noted that this approximated axis dynamically varies when the palm folds with the moving MCP joint. Here, we

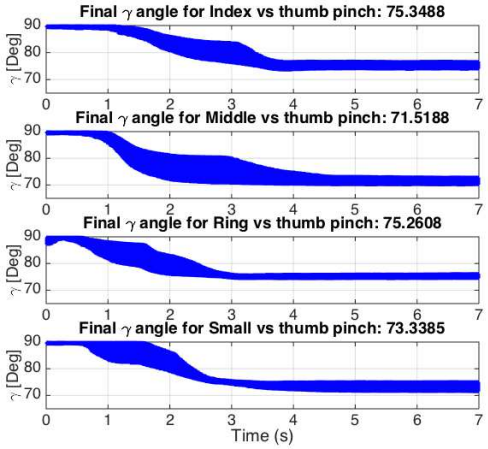

Fig. 6: Palm folding angle γ variation with each thumb-finger tip grasp posture combination across four subjects. Final average γ angle values for each thumb-finger interaction posture (Fig. 2) are marked along with the plots. Note the initial γ is 90° due to the palm axis assignment (Fig. 2(a))

.

argue that external assistive forces given at the MCP joint will have better efficacy if they are as perpendicular as possible to this palm folding axis.

3.2 Kinematic model simulations

A simplified kinematic model proposed in [12] is adopted to further understand how to maximize the efficacy of an external force given at the MCP joint to assist the grip force at the thumb tip by incorporating an approximation for the palm folding axis. Section 2.2 in methodology explains this model that accounts for palm folding and the thumb in detail.

The model based numerical simulation results for assistive force gains with respect to the assistive force directions $-50^\circ < \psi < 50^\circ$ at the MCP joint for different palm joint axis inclinations $50^\circ < \gamma < 80^\circ$ are shown in Fig. 7. In these figures, the variation of γ in the simplified biomechanical model represent a possible variation of the palm folding angle for different thumb-finger pairs. Numerical simulation results shown in Figs. 7(a) and 7(b) show that γ varies around 70° for maximum force gain at the thumb-tip. Therefore our simplified kinematic model prediction agrees with the experimental approximation of the steady state γ angle in Fig. 6.

Fig. 7(b) further shows that the maximum assistive force gain ratio of 1:1.6 can be obtained for an initial 1 N force at the thumb-tip when ψ is in the range $10^\circ < \psi < 20^\circ$ for $70^\circ < \gamma < 75^\circ$. These numerical simulation results in Fig. 7 suggests that assistive force direction ψ corresponding to the maximum assistive force gain (as indicated by the colour code) increases with increasing γ, confirming our original argument that the

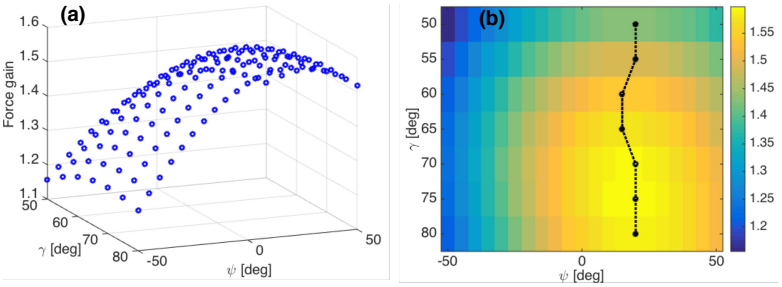

Fig. 7: (a) Assistive force gains at the thumb-tip for the assistive unit forces at the MCP joint calculated using thumb kinematics in Fig. 3 plotted against assistive force directions ($-50^\circ < \psi < 50^\circ$) and palm folding angle ($50^\circ < \gamma < 80^\circ$). (b) Maximum thumb-tip assistive force gains from Fig. 7(a) (connected in black dashed lines) with ψ and γ variations.

efficacy of an external assistive force at MCP joint can be optimized by having it as perpendicular to the palm folding axis as possible.

3.3 Thumb assistive force direction across the thumb-finger pairs (experiment 2)

Experiments are conducted on human subjects to test how far the model based prediction holds when the actual palm folding does not follow a strict linear axis and when the TM joint in practice does not strictly follow a simple three orthogonal axes model. Please see the details of experiment-2 in section 2.3 in methods.

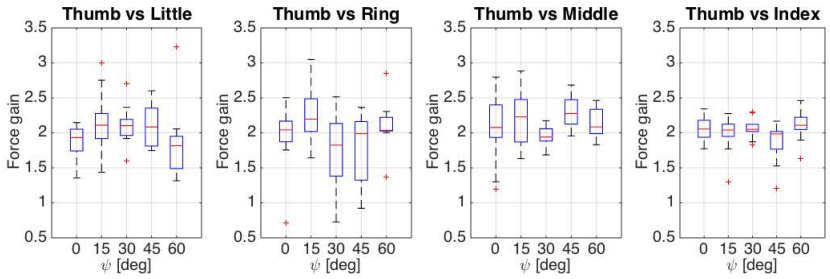

Fig. 8: Boxplots of thumb-tip assistive force gain for the linear actuator assistive force at the MCP joint in pinch grasp with each finger. Each box displays force gain values for an assistive tendon force direction in the range $0^\circ < \psi < 60^\circ$ (Fig. 4) for the ten subjects. $\psi = 60^\circ$ is the tendon closest to the index finger.

Fig. 8 shows boxplots of experimental assistive force gains for the assistive tendon directions ψ at the MCP joint for each thumb-finger pair across the ten subjects and five tendon directions. Since the force gain data for all finger-tendon pairs is not normally

Table 2: Comparison of the median force gains in Fig. 8 across the ten subjects for the assistive force directions $0^\circ < \psi < 60^\circ$ using non-parametric Wilcoxon rank sum right-tailed, left-tailed, and two-sided hypothesis tests (equivalent to Mann-Whitney U test). F_g^i - Median force gain for the assistive tendon direction, $\psi = i$ (Fig. 4) from the ulnar direction where $i = 0^\circ, 15^\circ, 30^\circ, 45^\circ, 60^\circ$. Statistically significant p-values (< 0.05) are noted with a * mark. Since $\psi = 0^\circ$ is not significantly different from any of the tendon directions corresponding p-values are not included in the table.

Thumb-finger pair	Wilcoxon rank sum test	Result	p-value
Thumb-little:			
	$F_g^{60^\circ} < F_g^{15^\circ}$	true	$0.0378^* (< 0.05)$
	$F_g^{60^\circ} < F_g^{30^\circ}$	true	$0.0129^* (< 0.05)$
	$F_g^{60^\circ} < F_g^{45^\circ}$	true	$0.027^* (< 0.05)$
	$F_g^{15^\circ} \neq F_g^{30^\circ}$	false	$0.9698\ (> 0.05)$
	$F_g^{15^\circ} \neq F_g^{45^\circ}$	false	$0.9698\ (> 0.05)$
	$F_g^{30^\circ} \neq F_g^{45^\circ}$	false	$0.9698\ (> 0.05)$
Thumb-ring:			
	$F_g^{30^\circ} < F_g^{15^\circ}$	true	$0.0226^* (< 0.05)$
	$F_g^{45^\circ} < F_g^{15^\circ}$	true	$0.032^* (< 0.05)$
Thumb-middle:			
	$F_g^{45^\circ} > F_g^{30^\circ}$	true	$0.0014^* (< 0.05)$
	$F_g^{45^\circ} \neq F_g^{60^\circ}$	false	$0.3075\ (> 0.05)$
	$F_g^{45^\circ} \neq F_g^{15^\circ}$	false	$0.7913\ (> 0.05)$
Thumb-index:			
	$F_g^{45^\circ} < F_g^{30^\circ}$	true	$0.0445^* (< 0.05)$
	$F_g^{60^\circ} > F_g^{45^\circ}$	true	$0.0226^* (< 0.05)$
	$F_g^{30^\circ} \neq F_g^{60^\circ}$	false	$0.4274\ (> 0.05)$
	$F_g^{15^\circ} \neq F_g^{60^\circ}$	false	$0.3847\ (> 0.05)$
	$F_g^{15^\circ} \neq F_g^{30^\circ}$	false	$0.6232\ (> 0.05)$

distributed ($p > 0.05$ Kolmogorov-Smirnov test), non-parametric Wilcoxon rank sum hypothesis test is performed to compare the median force gains.

Table 2 summarizes the outcome across the ten subjects. It shows that the median assistive force gains at $\psi = 15^\circ$, 30° and 45° are statistically significantly higher than that of $\psi = 60^\circ$ for the thumb-little pair. Moreover, a paired rank sum test confirms that the medians of $\psi = 15^\circ$, 30° and 45° are not significantly different indicating it is effective to apply forces in any angle between 15° and 45° for the thumb-little pair. $\psi = 15^\circ$ is the most effective for the thumb-ring pair. For the thumb-middle pair, median force gain at $\psi = 45^\circ$ is significantly higher than that of $\psi = 30^\circ$. A paired rank sum test confirms that the medians of $\psi = 45^\circ$, $\psi = 60^\circ$ pair and $\psi = 45^\circ$, $\psi = 15^\circ$ pair are not significantly different from each other. Hence the tendon directions greater or lower than 30° are the most effective for the thumb-middle pair. Significantly lower median force gain at $\psi = 45^\circ$ for the thumb-index pair than $\psi = 30^\circ$ and $\psi = 60^\circ$ and no significant difference among $\psi = 15^\circ$, 30° and 60°, indicates that thumb-index pair can be effectively supported by tendons at $\psi = 15^\circ$ and $\psi = 30^\circ$ directions. Since $\psi = 0^\circ$ is not significantly different from any of the directions and all the thumb-finger pairs are favoured by tendon angle directions $< 30^\circ$, it can be noted that $0^\circ < \psi < 30^\circ$ is the most effective for all the thumb-finger pairs.

4 Discussion

Our statistical analysis on experimental data confirms the model predictions by identifying the most effective asistive force direction in the range $0^\circ < \psi < 30^\circ$ (Table 2). Multiway Analysis of Variance (ANOVA) of experimental data from ten human subjects too confirm that there is a significant interaction effect between finger pairs (representing γ) and $30^\circ < \psi < 60^\circ$ ($p = 0.023$, $F = 2.76$) while there is no significant interaction effect when $0^\circ < \psi < 30^\circ$ ($p = 0.135$, $F = 1.72$). The variability of force gain across subjects (Fig. 8) can come from thumb anatomical variations [17].

In this work, we consider the initial ψ to build a relationship among ψ, γ, and the thumb-tip force gain. However, ψ changes with the thumb movement. Therefore, from a designer's point of view, knowing the best starting tendon angle would be practically more useful than the final angle that can vary depending on grasp affordances. In our experiment, palm folding angle γ is evaluated assuming that the palmar arches involve palm folding in straight axes [16]. According to the experiment results, average γ angles variation between 71.5° to 75.3° could be due to the size of the palmar muscles of each individual. The γ variations depending on the time (see Fig. 6) may be due to the subjectwise thumb moving strategies to reach each finger tip.

These findings are useful not only for the tendon actuated assistive devices but also for all the actuation mechanisms because the effective direction of actuation is significant to give assistance to the thumb. In the future, it will be interesting to investigate different types of methods to exert assistive forces in control directions such as exoskeletons, both hard [1] and soft [15].

5 Conclusion

Experimental results show that average palm folding angle varies from 71.5° to 75.3° across the four thumb-finger pairs for four subjects. Our numerical results based on the kinematic model of the thumb and the palm predict that the thumb-tip assistive force gain can be maximized by exerting assistive force vectors to the MCP joint in the range $10^\circ - 30^\circ$ from the ulnar axis, for palm folding angle in the range $70^\circ - 80^\circ$ from the radial axis in the coronal plane. This practically means that assistive forces at the MCP joint exerted perpendicular to the palm folding axis maximises the force gain at the thumbtip.

Statistical significance tests on experimental thumbtip force gain data show that the effective assistive force direction at the MCP is $0^\circ < \psi < 30^\circ$ across thumb-finger pairs for ten human subjects. This shows that the moment arm produced by the MCP assistive force around the palm folding axis plays a vital role in thumb tip force gain. This finding also indicates the significance of including foldable palm as an integral part of the kinematic model of the thumb to abstract thumb biomechanics to design assistive devices for the hand.

References

1. Aubin, P.M., Sallum, H., Walsh, C., Stirling, L., Correia, A.: A pediatric robotic thumb exoskeleton for at-home rehabilitation: The Isolated Orthosis for Thumb Actuation (IOTA). In: IEEE International Conference on Rehabilitation Robotics (ICORR). pp. 1–6 (2013)
2. Cempini, M., Cortese, M., Vitiello, N.: A powered finger–thumb wearable hand exoskeleton with self-aligning joint axes. IEEE/ASME Transactions on Mechatronics **20**(2), 705–716 (2015)
3. Chang, L.Y., Matsuoka, Y.: A kinematic thumb model for the act hand. In: IEEE International Conference on Robotics and Automation (ICRA). pp. 1000–1005 (2006)
4. Colditz, J.C.: The biomechanics of a thumb carpometacarpal immobilization splint: design and fitting. Journal of Hand Therapy **13**(3), 228–235 (2000)
5. Cotugno, G., Althoefer, K., Nanayakkara, T.: The role of the thumb: Study of finger motion in grasping and reachability space in human and robotic hands. IEEE Transactions on Systems, Man, and Cybernetics **47**(7), 1061–1070 (2016)
6. Craig, J.J.: Introduction to robotics: mechanics and control. vol. 3. Upper Saddle River: Pearson Prentice Hall (2005)
7. De Monsabert, B.G., Rossi, J., Berton, E., Vigouroux, L.: Quantification of hand and forearm muscle forces during a maximal power grip task. Medicine & Science in Sports & Exercise **44**(10), 1906–1916 (2012)
8. Diftler, M., Ihrke, C., Bridgwater, L., Davis, D., Linn, D., Laske, E., Ensley, K., Lee, J.: Roboglove - a robonaut derived multipurpose assistive device. IEEE International Conference on Robotics and Automation (ICRA) (2014)
9. Feix, T., Romero, J., Schmiedmayer, H.B., Dollar, A.M., Kragic, D.: The grasp taxonomy of human grasp types. IEEE Transactions on Human-Machine Systems **46**(1), 66–77 (2016)
10. Kang, B.B., Lee, H., In, H., Jeong, U., Chung, J., Cho, K.J.: Development of a polymer-based tendon-driven wearable robotic hand. In: IEEE International Conference on Robotics and Automation (ICRA). pp. 3750–3755 (2016)
11. Ladd, A.L., Weiss, A.P.C., Crisco, J.J., Hagert, E., Wolf, J.M., Glickel, S.Z., Yao, J.: The thumb carpometacarpal joint: anatomy, hormones, and biomechanics. Instructional course lectures **62**, 165–179 (2013)
12. Nanayakkara, V., Ataka, A., Venetsanos, D., Duran, O., Vitzilaios, N., Nanayakkara, T., Sahinkaya, M.N.: Kinematic analysis of the human thumb with foldable palm. In: 17th Conference Towards Autonomous Robotic Systems (TAROS). pp. 226–238. Springer (2016)
13. Nanayakkara, V.K., Cotugno, G., Vitzilaios, N., Venetsanos, D., Nanayakkara, T., Sahinkaya, M.N.: The role of morphology of the thumb in anthropomorphic grasping: A review. Frontiers in Mechanical Engineering **3**(5) (2017). https://doi.org/10.3389/fmech.2017.00005, http://journal.frontiersin.org/article/10.3389/fmech.2017.00005
14. Neumann, D.A., Bielefeld, T.: The carpometacarpal joint of the thumb: stability, deformity, and therapeutic intervention. Journal of Orthopaedic & Sports Physical Therapy **33**(7), 386–399 (2003)
15. Polygerinos, P., Wang, Z., Galloway, K.C., Wood, R.J., Walsh, C.J.: Soft robotic glove for combined assistance and at-home rehabilitation. Robotics and Autonomous Systems **73**, 135–143 (2015)
16. Sangole, A.P., Levin, M.F.: Arches of the hand in reach to grasp. Journal of biomechanics **41**(4), 829–837 (2008)
17. Santos, V.J., Valero-Cuevas, F.J.: Reported anatomical variability naturally leads to multimodal distributions of denavit-hartenberg parameters for the human thumb. IEEE Transactions on Biomedical Engineering **53**(2), 155–163 (2006)

18. Valero-Cuevas, F.J., Johanson, M.E., Towles, J.D.: Towards a realistic biomechanical model of the thumb: the choice of kinematic description may be more critical than the solution method or the variability/uncertainty of musculoskeletal parameters. Journal of biomechanics **36**(7), 1019–1030 (2003)
19. Wu, J.Z., Sinsel, E.W., Gloekler, D.S., Wimer, B.M., Zhao, K.D., An, K.N., Buczek, F.L.: Inverse dynamic analysis of the biomechanics of the thumb while pipetting: a case study. Medical Engineering & Physics **34**(6), 693–701 (2012)
20. Xiloyannis, M., Cappello, L., Khanh, D.B., Yen, S.C., Masia, L.: Modelling and design of a synergy-based actuator for a tendon-driven soft robotic glove. In: 6th IEEE International Conference on Biomedical Robotics and Biomechatronics (BioRob). pp. 1213–1219 (2016)